Model Predictive 2DOF PID Control for Slip Suppression of Electric Vehicles

Tohru Kawabe
Faculty of Engineering, Information and Systems, University of Tsukuba, Tsukuba 305-8573, Japan

Keywords: Electric vehicle, Slip ratio, Model predictive control, PID control, Two degrees of freedom.

Abstract: This paper propose the design method of 2DOF (two degrees of freedom) PID (Proportional-Integral-Derivative) controller based on MPC (Model predictive control). This controller is called as MP-2DOF PID controller. The method repeatedly optimizes the control parameters for each control period by solving an optimization problem based on the MPC algorithm, while using the 2DOF PID controller structure. Generally 2DOF PID controller can be implemented by a simple extension of the pre-existing PID controller with feed-forward element. This means we can get better performance without much cost. The proposed method aims to improve the maneuverability, the stability and the low energy consumption of EVs (Electric Vehicles) by controlling the wheel slip ratio. There also include numerical simulation results to demonstrate the effectiveness of the method.

1 INTRODUCTION

Recently EVs (Electric Vehicles) have received much attention, because they are one of the powerful solutions against the environment and energy problems (Brown et al., 2010; Mousazadeh et al., 2009; Hirota et al., 2011).

EVs are automobiles which are propelled by electric motors, using electrical energy stored in batteries or another energy storage devices. Electric motors have several advantages over ICEs (Internal-Combustion Engines):

(A) Energy efficient.

(B) Environmentally friendly.

(C) Performance benefits.

(D) Reduce energy dependence.

The travel distance per charge for EV has been increased through battery improvements and using regeneration brakes, and attention has been focused on improving motor performance. The following facts are viewed as relatively easy ways to improve maneuverability and stability of EVs.

- The input/output response is faster than for gasoline/diesel engines.
- The torque generated in the wheels can be detected relatively accurately
- Vehicles can be made smaller by using multiple motors placed closer to the wheels.

Much research has been done on the stability of general automobiles, for example, ABS (Anti-lock-Braking Systems), TCS (Traction-Control-Systems), and ESC (Electric-Stability-Control)(Zanten et al., 1995) as well as VSA (Vehicle-Stability-Assist)(Kin et al., 2001) and AWC (All-Wheel-Control) (Sawase et al., 2006). What all of these have in common is that they maintain a suitable tire grip margin and reduce drive force loss to stabilize the vehicle behavior and improve drive performance. With gasoline/diesel engines, however, the response time from accelerator input until the drive force is transmitted to the wheels is slow and it is difficult to accurately determine the drive torque, which limits the vehicle's control performance.

When the vehicle is starting off or accelerating, particularly on a slippery or wet road surface, the wheel spins easily, which causes unstable driving situation and large waste of energy. Therefore, it's important to keep the optimal driving force in all driving situation for motion stability and saving energy. During acceleration, the driving force of wheel directly depends on the friction coefficient between road and tire, which is in accordance with the wheel slip and road conditions. For this reason, it becomes possible to give the adequate driving force by controlling the wheel traction.

Kawabe T..
Model Predictive 2DOF PID Control for Slip Suppression of Electric Vehicles.
DOI: 10.5220/0004996700120019
In *Proceedings of the 11th International Conference on Informatics in Control, Automation and Robotics* (ICINCO-2014), pages 12-19
ISBN: 978-989-758-040-6

EVs have a fast torque response and the motor characteristics can be used to accurately determine the torque, which makes it relatively easy and inexpensive to realize high-performance traction control. This is expected to improve the maneuverability and stability of EV. It's, therefore, important to research and development to achieve high-performance EV traction control. Several methods have been proposed for the traction control (Fujii and Fujimoto, 2007) by using slip ratio of EVs, such as the method based on MFC (Model Following Control) in (Hori, 2000) and SMC (Sliding Mode Control) method (Li et al., 2012) by us. Moreover, we have been also proposed MP-PID (Model Predictive Proportional-Integral-Derivative) method in (Kawabe et al., 2011).

This method determines the PID controller gain using an MPC algorithm to utilize the capability of explicitly considering the constraints, which is one of the advantages of MPC, to achieve a more advanced and flexible control method(Maciejowski, 2005; Camacho and Bordons, 2004). Specifically, the optimum control input is calculated by the MPC explicitly considering the constraints and the PID gain for realizing this is derived in advance newline and used.

PID controllers have a simple construction and have been proved to be practical and highly reliable in many industrial fields(Astrom and Hagglund, 2005). Also many PID based control methods have been developed until now(Besancon-Voda, 1998; Precup and Preitl, 2006; Ginter and Pieper, 2011; Jin and Liu, 2014).

One of the merits of our proposed MP-PID control method is that the acknowledges acquired about conventional PID controller could be used.

Furthermore, MP-PID controller can be implemented smoothly from conventional PID controller since it still holds PID controller structure. However, there is still room for improving control performance of MP-PID control, especially target-tracking performance, in comparison to standard MPC.

This paper, therefore, proposes MP-2DOF PID (model predictive two-degree-of-freedom PID) control method. The method repeatedly optimizes the control parameters for each control period by solving an optimization problem based on the MPC algorithm, while using the 2DOF PID controller structure. 2DOF PID controller can be implemented by a simple extension of the pre-existing PID controller with feedforward element. This means MP-2DOF PID inherits the merits of MP-PID, and we can get better performance without much cost. The numerical examples show the effectiveness of the proposed method.

2 PRELIMINARIES

2.1 MPC

MPC has been attracted more attention in recent years. MPC can treat the constraint explicitly when the optimal input is calculated by repeating for each control period(Maciejowski, 2005).

MPC algorithm is to decide the optimal manipulated values which converge MPC the controlled values to reference values by iteration of optimizing a cost function under constraints. To take advantage of the modern control theory, MPC mainly use the state space model to describe the controlled object.

The outline of MPC algorithm is shown as fig.1.

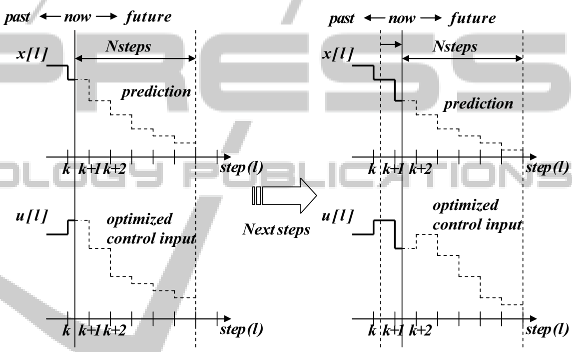

Figure 1: The outline of MPC.

At current time-step k controlled variables $x(k)$ is measured, and MPC controller predict the behavior of the controlled variables sequence from $\hat{x}(k+1)$ to $\hat{x}(k+H_p)$ by the dynamic model of the controlled object described as eqs. (1) and (2).

$$\begin{aligned} x(k+1) &= Ax(k)+Bu(k) && (1)\\ y(k) &= Cx(k) && (2) \end{aligned}$$

The behavior of system depends on future manipulated variables sequence from $\hat{u}(k)$ to $\hat{u}(k+Hp-1)$, that is why MPC controller calculate the sequence U = $[u(k), u(k+1), \cdots, u(k+H_P-1)]$ which makes desired behavior from perspective of cost-minimizing. After calculating, only $\hat{u}(k)$ is inputted to controlled object as current actual input, then, at the next time-step the plant state is sampled again and the prediction and the calculation are repeated. Where H_p is so-called predictive horizon and ˆ denotes a predictive value at k.

The cost function $J(k)$ at current time-step is given by

$$J(k) = \sum_{i=0}^{H_p-1} \left\{ \| \hat{x}(k+i+1) - x^d \|_Q^2 + \| \hat{u}(k+i) \|_R^2 \right\}. \quad (3)$$

The optimization problem with constraints is given by

$$\min_{U} J(k) \tag{4}$$

subject to

$$\begin{aligned} x_{min} &\leq \hat{x}(k+i) \leq x_{max} \\ u_{min} &\leq \hat{u}(k+i) \leq u_{max} \\ &\qquad i = 0,1,\cdots,Hp. \end{aligned} \tag{5}$$

We assume the controlled object is a multi-input multi-output system, thus $x(k)$ and $u(k)$ are vectors with adequate dimensions. $\| x \|_Q^2$ denotes the quadratic form $x^T Qx$, and x^d reference value and where Q and R are weighting matrices.

2.2 2 DOF PID Control

PID is an acronym created from Proportional (proportional action), Integral (integral action), and Derivative (derivative action), and it has a simple structure that makes it easy to intuitively understand the role of each action and thus has been used for many years in a variety of fields and today remains a proved, highly reliable control device used for a variety of subjects.

The control input generated by the standard 1 DOF PID controller in continuous-time is generally expressed by eq. (6).

$$u(t) = K_P e(t) + K_I \int_0^t e(\tau)d\tau + K_D \frac{de(t)}{dt} \tag{6}$$

where $e(t) := r(t) - y(t)$ (deviation), and where K_P, K_I, and K_D are called the proportional gain, integral gain, and differential gain, respectively.

As well known, the 2DOF control system naturally has generally advantages over the 1DOF control system. Various 2DOF PID controllers have been proposed for industrial use and also detailed analysis have been made including equivalent transformations, interrelationship with previously proposed variation of 1DOF PID (i.e., the preceded-derivative PID and the I-PD) controllers until now (Araki and Taguchi, 2003).

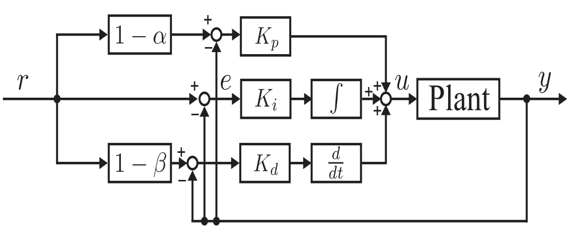

Figure 2: 2DOF PID control system.

Although there are various form of 2DOF PID controller, one of the simple form as shown in fig.2 is employed in this paper. Where α $(0 \leq \alpha \leq 1)$ and β $(0 \leq \beta \leq 1)$ are feed forward gains.

The control input by this 2DOF PID controller in discrete-time is expressed as follows.

$$\begin{aligned} u(k) &= K_P[(1-\alpha)e(k)] \\ &\quad + K_I\left[\sum_{i=0}^{k} e(i)\right] \\ &\quad + K_D[(1-\beta)(e(k)-r(k-1))+y(k-1)] \end{aligned} \tag{7}$$

3 ELECTRIC VEHICLE DYNAMICS

As a first step toward practical application, this paper restricts the vehicle motion to the longitudinal direction and uses direct motors for each wheel to simplify the one-wheel model to which the drive force is applied. In addition, braking was not considered this time with the subject of the study being limited to only when driving.

From fig. 3, the vehicle dynamical equations are expressed as eqs. (8) to (11).

$$M\frac{dV}{dt} = F_d(\lambda) - F_a - \frac{T_r}{r} \tag{8}$$

$$J\frac{d\omega}{dt} = T_m - rF_d(\lambda) - T_r \tag{9}$$

$$F_m = \frac{T_m}{r} \tag{10}$$

$$F_d = \mu(c,\lambda)N \tag{11}$$

Where M is the vehicle weight, V is the vehicle body velocity, F_d is the driving force, J is the wheel inertial moment, F_a is the resisting force from air resistance and other factors on the vehicle body, T_r is the frictional force against the tire rotation, ω is the wheel angular velocity, T_m is the motor torque, F_m is the motor torque force conversion value, r is the wheel radius, and λ is the slip ratio. The slip ratio is defined by (12) from the wheel velocity (V_ω) and vehicle body velocity (V).

$$\lambda = \begin{cases} \dfrac{V_\omega - V}{V_\omega} & \text{(accelerating)} \\ \dfrac{V - V_\omega}{V} & \text{(braking)} \end{cases} \tag{12}$$

λ during accelerating can be shown by (13) from fig. 3.

$$\lambda = \frac{r\omega - V}{r\omega} \tag{13}$$

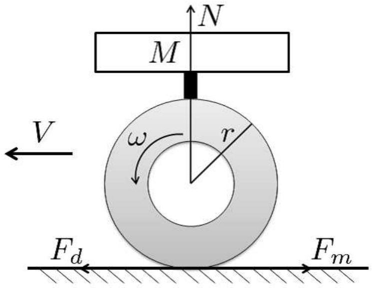

Figure 3: One-wheel car model.

The frictional forces that are generated between the road surface and the tires are the force generated in the longitudinal direction of the tires and the lateral force acting perpendicularly to the vehicle direction of travel, and both of these are expressed as a function of λ. The frictional force generated in the tire longitudinal direction is expressed as μ, and the relationship between μ and λ is shown by (14) below, which is a formula called the Magic-Formula(Pacejka and Bakker, 1991) and which was approximated from the data obtained from testing.

$$\mu(\lambda) = -c_{road} \times 1.1 \times (e^{-35\lambda} - e^{-0.35\lambda}) \qquad (14)$$

Where c_{road} is the coefficient used to determine the road condition and was found from testing to be approximately $c_{road} = 0.8$ for general asphalt roads, approximately $c_{road} = 0.5$ for general wet asphalt, and approximately $c_{road} = 0.12$ for icy roads. For the various road conditions $(0 < c < 1)$, the $\mu - \lambda$ surface is shown in fig. 4.

It shows how the friction coefficient μ increases with slip ratio λ $(0.1 < \lambda < 0.2)$ where it attains the maximum value of the friction coefficient. As defined in (11), the driving force also reaches the maximum value corresponding to the friction coefficient. However, the friction coefficient decreases to the minimum value where the wheel is completely skidding. Therefore, to attain the maximum value of driving force for slip suppression, it should be controlled the optimal

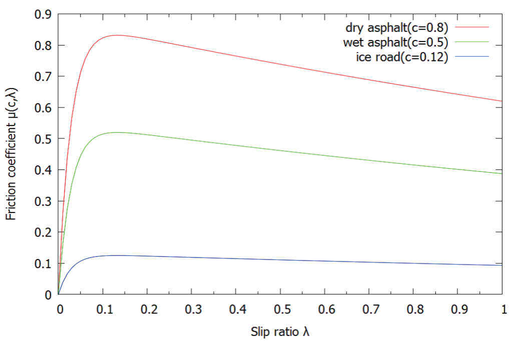

Figure 4: λ-μ surface for road conditions.

value of slip ratio. the optimal value of λ is derived as follows. Choose the function $\mu_c(\lambda)$ defined as

$$\mu_c(\lambda) = -1.1 \times (e^{-35\lambda} - e^{-0.35\lambda}). \qquad (15)$$

By using eqs. (14) and (15), it can be rewritten as

$$\mu(c, \lambda) = c_{road} \cdot \mu_c(\lambda). \qquad (16)$$

Evaluating the values of λ which maximize $\mu(c, \lambda)$ for different $c(c > 0)$, means to seek the value of λ where the maximum value of the function $\mu_c(\lambda)$ can be obtained. Then let

$$\frac{d}{d\lambda}\mu_c(\lambda) = 0 \qquad (17)$$

and solving equation (17) gives

$$\lambda \;=\; \frac{log100}{35 - 0.35} \approx 0.13. \qquad (18)$$

Thus, for the different road conditions, when $\lambda \approx 0.13$ is satisfied, the maximum driving force can be gained. Namely, from (14) and fig. 4, we find that regardless of the road condition (value of c), the $\lambda - \mu$ surface attains the largest value of μ when λ is the optimal value 0.13.

4 MP-2DOF PID CONTROL

There is a difference in the control structure between PID and MPC. Compared to PID controller whose input is determined by the PID gains, MPC is based on the state-space feedback controller and optimizes the control input directly at each step. As a result, MP-PID control method has been proposed(Kawabe et al., 2011). This method applies MPC algorithm to design the PID controller gains. Specifically, the optimum control input which is calculated by the MPC explicitly considering the constraints is converted to the three PID gains at each step.

However, there is still room for improving control performance of MP-PID control, especially target-tracking performance. Therefore, in this research, to extend the MP-PID controller to the MP-2DOF PID controller. For tuning the parameters of 2DOF PID controller by the MPC algorithm, the control input eq.(7) is rewritten as follows.

$$\begin{aligned}
\hat{u}(k+j) = {} & K_P\,[(1-\alpha)r(k+j) - \hat{y}(k+j)] \\
& + K_I \left[\sum_{l=0}^{k} e(l) + \sum_{l=1}^{j} \hat{e}(k+l)\right] \\
& + K_D[(1-\beta)(r(k+j) - \hat{y}(k+j)) \\
& \quad - (1-\beta)r(k+j-1) + \hat{y}(k+j-1)]
\end{aligned} \qquad (19)$$

where

$$e(k) = r(k) - y(k) \qquad (20)$$

Then, the predictive value of $y(k+i)$ is expressed

$$\hat{y}(k+i) = CA^i x + \sum_{j=0}^{H_p-1} \left[CA^{i-1}B, \cdots, CB\right] \left[\hat{u}(k), \cdots, \hat{u}(k+i-1)\right]^T . \tag{21}$$

The 2DOF-PID controller is determined from Eqs. (19) by using the set of $\theta = (K_P\ K_I\ K_D\ \alpha\ \beta)$ including three feedback PID gains ($K_P,\ K_I,\ K_D$) and two forward gains (α, β),

For tuning of these five MP-2DOF PID gains, we need to solve an optimization problem to get the optimum θ. A weighted square sum with respect to e and u within the prediction horizon H_p is generally used as t he objective function. Here, the objective function J_{LQ} is given as

$$J_{LQ} = \sum_{i=1}^{H_p} q_i \hat{e}^2(k+i) + \sum_{j=0}^{H_p-1} r_j \hat{u}^2(k+j). \tag{22}$$

In Eq. (22), e is evaluated at each time-step $k, k+1, \cdots, k+H_p$ and u is evaluated at each control interval $k, k+N_c-1, k+2N_c-1, \cdots, k+H_p$. By using state space model, eqs.(1) and (2), repeatedly, we can express $\hat{r}(k+1), \cdots, \hat{r}(k+H_p)$, $\hat{y}(k+1), \cdots, \hat{y}(k+H_p)$, $\hat{e}(k), \cdots, \hat{e}(k+H_P)$, $\hat{u}(k), \hat{u}(k+H_p)$ and J_{LQ} by $\vec{\theta}$. As a result, the controller design problem at step k is formulated as follows,

$$\min_{\theta} J_{LQ}(\theta) \tag{23}$$

subject to Eqs. (20) and (21)

$$j = 0, \cdots, H_p-1; \quad i = 1, \cdots, H_p.$$

The proposed method is solved this problem eq. (23) on each step according to MPC algorithm by using some optimization method (for example, the grid search to the discretized θ). Once optimum θ at k is obtained, optimum $u(k) = \hat{u}(k)$ is calculated by eq. (19). The simulation results by this method for slip suppression control problem of EV are shown in the next section. We may note, in passing, that values of α and β are fixed to 0, it's standard 1DOF PID controller. The proposed method, therefore, includes 1DOF MP-PID controller design.

5 NUMERICAL EXAMPLES

5.1 Simulation Settings and Arrangements

This section shows the numerical simulation results to demonstrate the effectiveness of the proposed method as shown in previous section. Firstly, as shown by eqs. (8) $\sim$ (11), the vehicle model has nonlinear characteristics and it's difficult to apply the proposed method to this model as it is. Therefore, a linear approximated model as the perturbed system in the time ($t = k$) is used. If we use the slip ratio in the time $t = k$ as λ_k, and the $\lambda - \mu$ curve inclination in λ_k as

$$a = \left.\frac{d\mu}{d\lambda}\right|_{\lambda_k}, \tag{24}$$

and using eqs. (8) $\sim$ (11), the relation of variation of the slip ratio $\Delta\lambda$ and variation of the motor torque ΔT_m is expressed as follows.

$$\frac{\Delta\lambda}{\Delta T_m} = \frac{M(1-\lambda_k)}{aN\left[M(1-\lambda_k) + \dfrac{J}{r^2}\right]} \times \frac{1}{\tau_a s + 1} \tag{25}$$

where

$$\tau_a := \frac{J\omega M(1-\lambda_k)}{arN\left[M(1-\lambda_k) + \dfrac{J}{r^2}\right]} \tag{26}$$

The transfer function is numerically realized using the application software, $Matlab(Ver.8.1.0.604)$ as the continuous-time state space of the SISO (Single Input Single Output) system. Furthermore, the continuous-time state space model is transformed to the discrete-time state space model with the sampling time $T_s = 0.01$ sec. by $Matlab$.

The value of parameters used in the simulations are showed in Table 1, particularly, the value of vehicle mass is given to $1100kg$, including the sum of the mass of the car $1000kg$ and the loading weight (the weight of one passenger and luggage) $100kg$.

Table 1: Parameters used in the simulations.

M: Mass of vehicle	$1100[kg]$
J_w: Inertia of wheel	$21.1[kg/m^2]$
r: Radius of wheel	$0.26[m]$
λ^*: Reference slip ratio	0.13
g: Acceleration of gravity	$9.81[m/s^2]$

As the input to the simulation of system, the toque is produced by the constant pressure on the accelerator pedal, which makes the vehicle speed increased from 0 to approximately $72km/h$ in $10[s]$ on the dry asphalt surface. The variations in road condition coefficient c and mass of vehicle M are defined as follows.

$$c_{min}(=0.1) \quad \le c \le \quad c_{max}(=0.9)$$
$$M_{min}(=1000[kg]) \quad \le M \le \quad M_{max}(=1400[kg])$$

In addition to, the constrained conditions, $-1000 \le T_m \le 1000[Nm]$, $0 \le V_w \le 180[km/h]$ and $0 \le V \le 180[km/h]$ are added in the simulation.

5.2 Simulation Results

In order to verify the performance of the proposed method, we compare it with no control using two kinds of road conditions, the high friction road (dry asphalt) and the low friction roads (ice road) to make the simulation for comparison conveniently. For the dry asphalt, the road condition coefficient c value of 0.8 is chosen and for the ice road, c value of 0.12 is chosen.

5.2.1 Simulation 1: Variation in Road Condition with Fixed Vehicle Mass

Simulation 1 is performed to verify the performance of the proposed method with variation only in road condition (c) , namely the road condition varying but the vehicle mass is fixed. The results of Simulation 1 is shown by fig. 5. The results of the conventional 1DOF PID controller which gains designed by the standard Ziegler and Nichols method are also shown for comparison with the proposed 2DOF PID control.

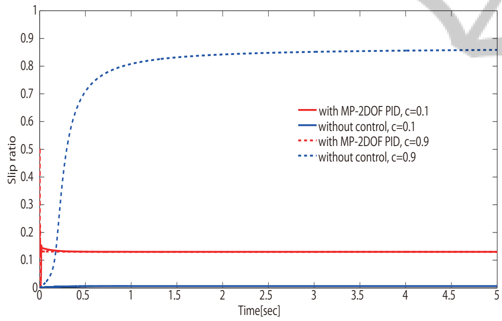

Figure 5: Time response of slip ratio with proposed MP-2DOF PID control and no control, $M = 1100[kg]$ ($c = 0.1$ and $c = 0.9$).

Fig. 5 shows the results of proposed method under the most severe conditions with $c = 0.1$ and $c = 0.9$ comparing with no control applied. The slip ratio can maintain to 0.13 regardless of the variation in c, on the contract, the slip ratio without control changes utterly. Hence, the proposed method takes a better performance than no control even with the variation happening in road surface condition.

5.2.2 Simulation 2: Moving from Dry Asphalt to Ice Road with Variation in The Vehicle Mass

In Simulation 2, the robustness of the proposed method with variation both in the road condition and vehicle mass is confirmed. For making the variation to the vehicle mass M is assigned to $1000[kg]$, $1200[kg]$ and $1400[kg]$ respectively. Two different roads are considered, a high friction road (dry asphalt) for $t \in [0.0, 3.0]s$ and a low friction road (ice road) for $t \in [3.0, 5.0]s$. The results of the conventional 1DOF PID controller which gains designed by the standard Ziegler and Nichols method are also shown for comparison with the proposed 2DOF PID control.

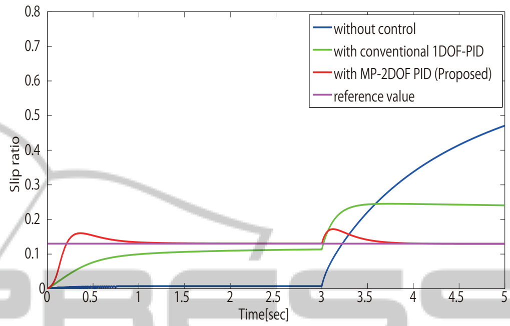

Figure 6: Time response of slip ratio ($M = 1000kg$).

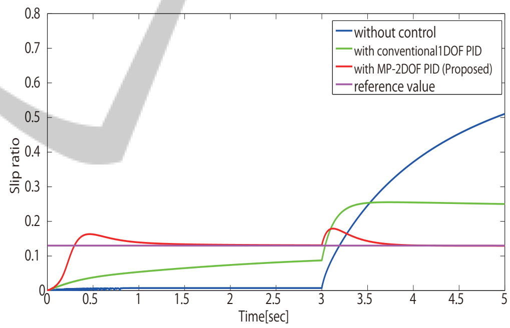

Figure 7: Time response of slip ratio ($M = 1200kg$).

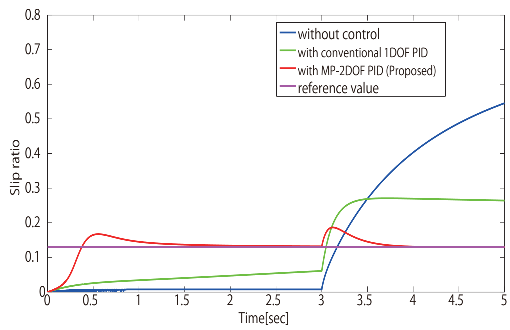

Figure 8: Time response of slip ratio ($M = 1400kg$).

From figs.6, 7 and 8, the slip ratio using the proposed method can maintain to the reference value 0.13 accurately, regardless of both of the road condition and the vehicle mass varying. That is to say, the

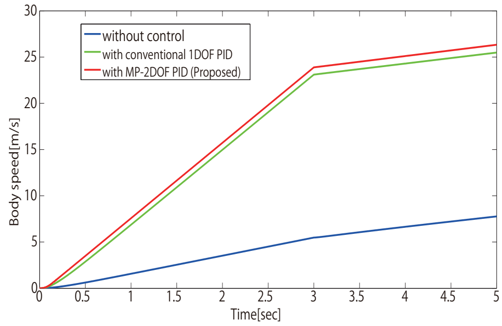

Figure 9: Time response of body speed ($M = 1000kg$).

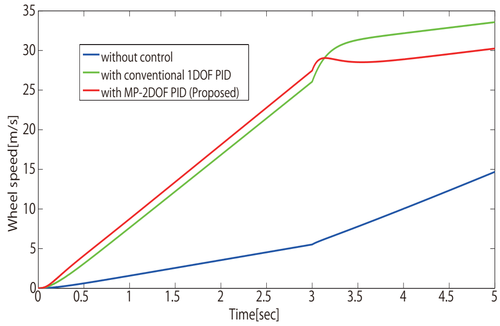

Figure 11: Time response of wheel speed ($M = 1000kg$).

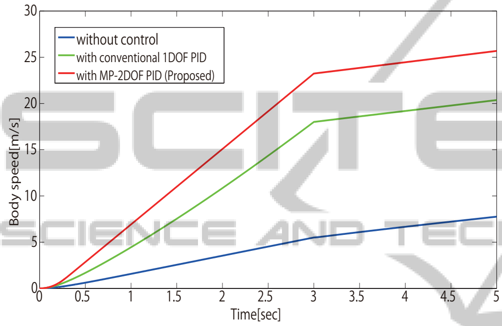

Figure 10: Time response of body speed ($M = 1400kg$).

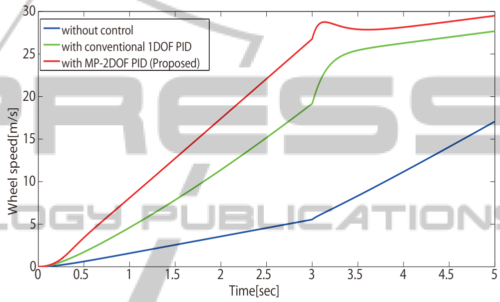

Figure 12: Time response of wheel speed ($M = 1400kg$).

proposed method performs strong robustness to the variation in the road condition and the vehicle mass. The transient performance and steady-state accuracy of the response of slip ratio will become weaker when the width of the boundary layer increases with the conventional 1DOF PID controller. However by using the proposed MP-2DOF PID controller, the disadvantages can be overcome.

For saving of space, only results with the case of vehicle mass M assigned to $1000[kg]$ and $1400[kg]$ are limited to shown below. (The results with $M = 1200[kg]$ are omitted.) From figs.9 $\sim$ 12, we can see that the vehicle can attain the best acceleration with the proposed method. These figs also show that the wheel speed can be restrained to attain better acceleration with the proposed method than using the 1DOF PID controller and no control.

As contrasted, the performance of the system with proposed MP-2DOF PID controller is much better than the system with the conventional 1DOF PID controller and no control. Moreover, in order to obtain the desired slip ratio on the high friction surface, it is necessary to produced more torque which can allow the car get better acceleration. That is, when the car travel on the high friction road, the high driving toque should be given to the wheel for better acceleration.

6 CONCLUSIONS

This paper proposes MP-2DOF PID control method for EV traction control. The control objective focused on suppressing the slip ratio to the desired value with the variation in the road condition and vehicle mass which allows the vehicle to get the maximum driving force during the acceleration. We can verified that the the proposed method shows good performance by comparing to conventional method. We can also confirm that it is an easy way to improve the control performance without much cost by expanding PID controller to 2DOF PID controller.

As future works, in this paper, the effectiveness of the proposed method for acceleration was only verified, for more attention, making the method effective for the deceleration should be considered. At last, there is much that is needed to be done for the energy conservation in the future. This paper was limited to show an example construction of the MP-2DOF PID control system that can reduce the drive loss using a simplified one wheel model in the case of acceleration, but to make the method practical, making the method effective for a variety of road conditions must be performed and also created the method using more detailed two-wheel and four-wheel models. In addition, the suitability of the proposed method must be studied not only for the slip suppression addressed by this paper but also for overall driving including during braking. Even for this issue, however, the basic framework of the proposed method can be used as is and can also be expanded relatively easily to form a foundation for making practical EV high performance traction control systems and promoting further progress.

ACKNOWLEDGEMENTS

This research was partially supported by Grant-in-Aid for Scientific Research (C) (Grant number: 24560538; Tohru Kawabe; 2012-2014) from the Ministry of Education, Culture, Sports, Science and Technology of Japan.

REFERENCES

Araki, M. and Taguchi, T. (2003). Two-degree-of freedom pid controllers. *International Journal of Control, Automation, and Systems*, 1(4):401–411.

Astrom, K. and Hagglund, T. (2005). *Advanced PID Control*. The Instrumentation, Systems, and Automation Society.

Besancon-Voda, A. (1998). Iterative auto-calibration of digital controllers. methodology and applications. *Control Engineering Practice*, 6(3):345–358.

Brown, S., Pyke, D., and Steenhof, P. (2010). Electric vehicles: The role and importance of standards in an emerging market. *Energy Policy*, 38(7):3797–3806.

Camacho, E. and Bordons, C. (2004). *Model Predictive Control: Advanced Textbooks in Control and Signal Processing*. Springer-Verlag.

Fujii, K. and Fujimoto, H. (2007). Slip ratio control based on wheel control without detection of vehiclespeed for electric vehicle. *IEEJ Technical Meeting Record*, VT-07-05:27–32.

Ginter, V. and Pieper, J. (2011). Robust gain scheduled control of a hydrokinetic turbine. *IEEE Transactions on Control Systems Technology*, 19(4):805–817.

Hirota, T., Ueda, M., and Futami, T. (2011). Activities of electric vehicles and prospect for future mobility. *Journal of The Society of Instrument and Control Engineering*, 50:165–170.

Hori, Y. (2000). Simulation of mfc-based adhesion control of 4wd electric vehicle. *IEEJ Record of Industrial Measurement and Control*, pages IIC–00–12.

Jin, Q. and Liu, Q. (2014). Imc-pid design based on model matching approach and closed-loop shaping. *ISA Transactions*, 53(2):462–473.

Kawabe, T., Kogure, Y., Nakamura, K., Morikawa, K., and Arikawa, K. (2011). Traction control of electric vehicle by model predictive pid controller. *Transaction of JSME Series C*, 77(781):3375–3385.

Kin, K., Yano, O., and Urabe, H. (2001). Enhancements in vehicle stability and steerability with vsa. *Proceedings of JSME TRANSLOG 2001*, pages 407–410.

Li, S., Nakamura, K., Kawabe, T., and Morikawa, K. (2012). A sliding mode control for slip ratio of electric vehicle. *Proceedings of SICE Annual Conference 2012*, pages 1974–1979.

Maciejowski, J. (2005). *Predictive Control with Constraints*. Tokyo Denki University Press (Trans. by Adachi,S. and Kanno,M.) (in Japanese).

Mousazadeh, H., Keyhani, A., Mobli, H., Bardi, U., Lombardi, G., and Asmar, T. (2009). Environmental assessment of ramses multipurpose electric vehicle compared to a conventional combustion engine vehicle. *Journal of Cleaner Production*, 17(9):781–790.

Pacejka, H. and Bakker, E. (1991). The magic formula tire model. *Vehicle system dynamics*, 21:1–18.

Precup, R. and Preitl, S. (2006). Pi and pid controllers tuning for integral-type servo systems to ensure robust stability and controller robustness. *Electrical Engineering*, 88(2):149–156.

Sawase, K., Ushiroda, Y., and Miura, T. (2006). Left-right torque vectoring technology as the core of super all wheel control (s-awc). *Mitsubishi Motors Technical Review*, 18:18–24.

Zanten, A., Erhardt, R., and Pfaff, G. (1995). Vdc; the vehicle dynamics control system of bosch. *Proceedings of Society of Automotive Engineers International Congress and Exposition 1995*, page Paper No. 950759.